(Received 26 October 2025, Accepted 26 November 2025, Scheduled 16 January 2026)

Design and Experimental Evaluation of a Compact Half-Shaped Printed-Monopole Antenna with Short Stub for UWB Systems

Nobuyasu Takemura*

Chukyo University, Japan

ABSTRACT: A compact, half-shaped, planar-monopole antenna optimized for ultra-wideband (UWB) communication systems was proposed, numerically analyzed, and experimentally validated. The proposed antenna is configured as a bell-shaped monopole structure fabricated on an FR-4 dielectric substrate, which is bisected along its axis of symmetry to achieve a reduced footprint. To ensure broadband impedance matching, a short-circuited stub is integrated between the monopole and the ground conductor through a plated via. The antenna dimensions are $30 \times 12 \times 1.6\,\text{mm}^3$, which represent a significant reduction compared with those of conventional UWB monopole antennas. Full-wave electromagnetic simulations demonstrate that the antenna covers the FCC-authorized UWB of 3.1–10.6 GHz with a voltage standing-wave ratio (VSWR) of ≤ 2. Experimental measurements of properties of a fabricated prototype of the proposed antenna agree well with the simulation results. In addition to the analysis of frequency-domain performance, time-domain analysis is conducted using two identical antennas in both face-to-face and side-by-side arrangements. According to the results of the time-domain analysis, the calculated correlation coefficient between signals received by the proposed antenna is 0.986, which confirms high waveform fidelity. Group-delay analysis of the proposed antenna verified stable temporal characteristics with an average delay of approximately 0.2 ns across the UWB range. These results demonstrate that the proposed antenna is a promising candidate for compact and high-performance integration in short-range high-speed wireless communication devices.

1. INTRODUCTION

Ultra-wideband (UWB) systems — which exploit an extremely wide frequency spectrum — have attracted considerable attention as a technology enabling high-speed, short-range wireless communications [1, 2]. Although UWB systems occupy a broad bandwidth, the power of the transmitted signal is sufficiently dispersed so as not to cause harmful interference to existing wireless services and thereby achieve "spectral coexistence". In 2002, the Federal Communications Commission (FCC) allocated the 3.1–10.6 GHz band for UWB operation. It thus became necessary to develop antenna designs with wideband impedance characteristics capable of covering that frequency range [3]. To be integrated into practical wireless devices, including personal computers, smartphones, and digital cameras, UWB antennas must be compact while simultaneously providing omnidirectional radiation characteristics to ensure reliable communication with terminals in arbitrary orientations [4].

A wide variety of planar antenna configurations for UWB systems have been investigated. They include bow-tie antennas printed on both sides of a substrate and circular monopole antennas [5, 6]. Bow-tie antennas can be regarded as planar manifestations of biconical antennas, which are inherently self-similar structures. Monopole antennas, on the contrary, are characterized by their structural simplicity and omnidirectional radiation properties, which make them suitable for numerous wireless communication applications. Planar monopole antennas with diverse geometries, such as circle, ellipse, rectangle, trapezoid, pentagon, and square, have been proposed for UWB operation [7–10]. Among these geometries, circular and elliptical monopole antennas have demonstrated superior broadband performance compared to other shapes [7]. In addition to geometrical optimization, several impedance matching strategies have been introduced for UWB monopole antennas. They include partial truncation of the monopole element, the use of dual-feed structures, trident-shaped feed lines, and microstrip lines of varying widths [10–13]. Such strategies have been shown to enhance impedance bandwidth substantially, in some cases achieving more than three times of the bandwidth obtained without impedance matching. More recently, research efforts have focused on miniaturization while preserving wideband characteristics. Reported approaches include sector-shaped and trapezoidal unbalanced dipole antennas, planar UWB antennas with corrugation, ring-slot, and tapered-slot structures, and wide-slot configurations [14–18]. Others include a U-shaped antenna using low-cost liquid crystal polymer (LCP) organic material, an asymmetric circular slotted semi-circle-shaped extended antenna, and a modified hexagonal shape antenna [19–21]. Furthermore, several notable compact UWB monopole antenna designs have been presented, such as notched-band printed monopoles [22], circularly-polarized UWB monopoles derived from characteristic mode analysis [23], defected ground structure (DGS)-based wideband monopoles [24], and characteristic-mode-based design approaches that improve radiation and

* Corresponding author: Nobuyasu Takemura (takemura@sist.chukyo-u.ac.jp).

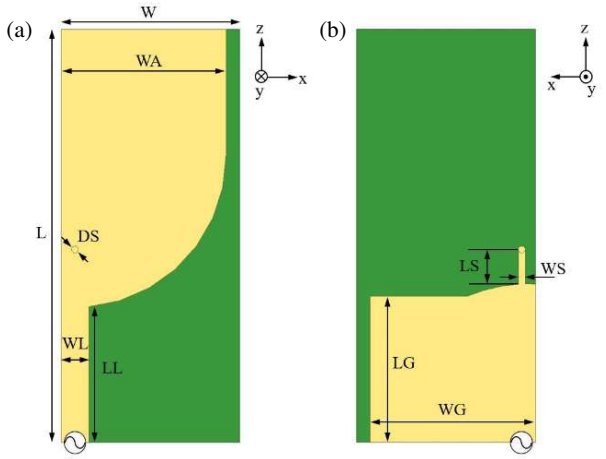

FIGURE 1. Antenna configuration: (a) front view and (b) back view.

polarization stability over wide frequency ranges [25]. These recent works demonstrate various strategies for improving UWB antenna performance, including multi-band rejection, modal optimization, ground-plane modification, and circular polarization synthesis. These designs successfully achieve impedance matching and exhibit satisfactory performance across the FCC-defined UWB spectrum of 3.1–10.6 GHz.

To address the challenge of miniaturizing UWB antennas, the authors previously proposed a bell-shaped planar monopole antenna incorporating a short-circuited stub to improve impedance matching at lower frequencies [26]. The introduction of the short stub enhances impedance matching at lower frequencies, thereby enabling broadband characteristics that satisfy the bandwidth requirements for UWB systems. The resulting antenna configuration achieves a compact form factor with overall dimensions of $28 \times 20 \times 1.6\,\text{mm}^3$.

In this study, a prototype UWB monopole antenna using a symmetrical configuration, which we previously proposed [27], was evaluated by time-domain analysis. The proposed UWB monopole antenna is bisected along its axis of symmetry, and impedance matching is achieved by appropriately tuning the dimensions of the short-circuited stub and the ground conductor. Specifically, the antenna is divided such that the microstrip feed line is retained, while the short stub facilitates impedance matching in the lower portion of the UWB frequency range.

Compared with our earlier study in [27], the present work offers several new technical advancements. First, we introduce a systematic parametric optimization framework for the half-shaped monopole, covering the ground-plane length, short-stub dimensions, and via diameter. These parameters were not fully examined in [27]. Second, we perform comprehensive time-domain evaluations, including waveform correlation and group-delay analysis. These evaluations were not included in the earlier study but are essential for assessing UWB pulse fidelity. Third, we quantitatively compare the half-shaped monopole with the full bell-shaped monopole reported in [26]. This comparison demonstrates that the half-shaped design preserves the entire UWB bandwidth (3.1–10.6 GHz) while reducing the antenna area by 36%. Finally, we present new experimental results, including measured omnidirectional radiation patterns, to validate the improved design.

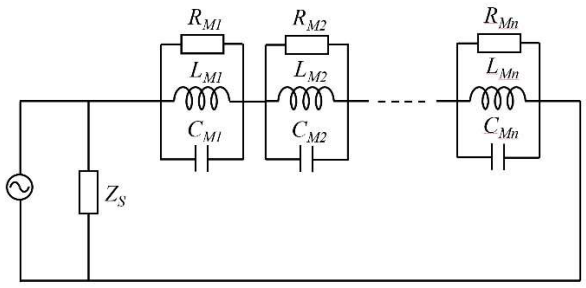

FIGURE 2. Equivalent circuit of half-shaped printed-monopole UWB antenna with a short stub.

The paper is organized as follows. Section 2 describes the configuration of the proposed antenna and its operating principle through parametric analysis. Section 3 presents the simulation results together with the results of an experimental validation using a fabricated prototype. Section 4 presents the results of an evaluation of time-domain performance, and Section 5 concludes the work.

2. ANTENNA DESIGN

The geometry of the proposed antenna is derived from the bell-shaped planar monopole antenna previously reported by the authors. In the earlier configuration, the bell-shaped monopole is directly printed on an FR-4 substrate, and impedance matching at lower frequencies is achieved by attaching a short stub. In this study, the symmetrical nature of that antenna is exploited by cutting the monopole along its axis of symmetry, resulting in a half-shaped monopole configuration. This approach substantially reduces the antenna's size while preserving the essential current distribution patterns that support broadband operation.

The configuration of the proposed half-shaped planar UWB monopole antenna incorporating a short-stub structure is shown in Figure 1. The antenna is formed on an FR-4 substrate ($\varepsilon_r = 4.4$, $\tan\delta = 0.02$) with dimensions of $L = 30\,\text{mm}$, $W = 12\,\text{mm}$, and $t = 1.6\,\text{mm}$. A bell-shaped monopole element and a microstrip feed line are patterned on the top surface of the substrate, while a partially circular ground plane (for enhancing impedance matching) and the short-stub line are implemented on the reverse side. The short stub extends from the lower edge of the monopole to the ground conductor and is connected to the monopole via a plated throughhole. Both the monopole and ground plane are configured in a half-shaped geometry. The antenna is designed for a characteristic impedance of $50\,\Omega$. The design intentionally leverages the structural symmetry of monopoles; that is, although only half of the original radiator is retained, introducing the short stub and partially circular ground ensures that the dominant resonant modes are preserved.

The equivalent circuit of the proposed UWB monopole antenna with a short stub is shown in Figure 2. The antenna can be modeled as a cascade of parallel resonant circuits [28], where each resonance is represented by resistance R_{Mk}, inductance L_{Mk}, and capacitance C_{Mk} ($k = 1, 2, \ldots, n$). The overlapping of these resonances produces an ultra-wideband impedance bandwidth. In this equivalent representation, the short stub is

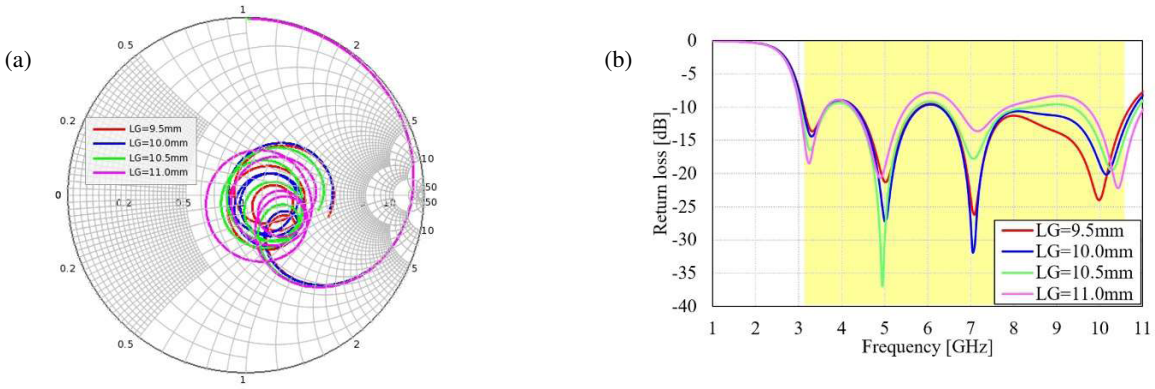

FIGURE 3. Calculated input impedance (with parameter LG): (a) Smith chart (1–11 GHz) and (b) reflection characteristic.

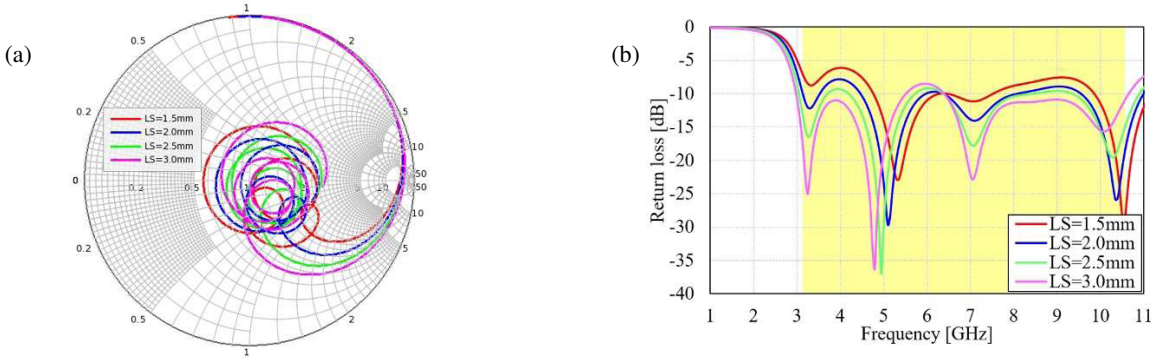

FIGURE 4. Calculated input impedance (with parameter LS): (a) Smith chart (1–11 GHz) and (b) reflection characteristic.

TABLE 1. Dimensional parameters of proposed antenna.

Parameter	L	W	LL	WL	WA
Length [mm]	30.0	13.0	10.0	2.0	12.0
Parameter	LS	WS	DS	LG	WG
Length [mm]	2.5	0.5	0.5	10.5	12.0

modeled as an additional parallel impedance Z_S connected to the monopole. By tuning the dimensions of the stub, it is possible to adjust Z_S and control the input impedance of the antenna, which can be tuned to improve input impedance matching, particularly at lower frequencies. By modifying the physical dimensions of the stub, it is possible to control the stub's impedance and thereby broaden the operational bandwidth of the antenna when the stub's impedance is combined with the inherent resonances of the monopole. The partially circular ground conductor further contributes to impedance matching. Note that the equivalent circuit in Figure 2 is a conceptual model that interprets the dominant resonance behavior, not a quantitative reproduction of the antenna's full electromagnetic response. Due to the complex, three-dimensional current distribution and the multiple, higher-order resonances excited in the half-shaped monopole with a short stub, an exact circuit realization that fully matches the broadband EM characteristics would require an extensive, multi-resonance network. The present circuit representation is intended to provide an understanding of how the short stub contributes to impedance matching. The key design parameters of the antenna include the length (LL) and width (WL) of the feedline, monopole width (WA), stub length (LS) and width (WS), through-hole diameter (DS), and ground-plane length (LG) and width (WG). The reference values of these parameters are summarized in Table 1. The antenna is designed to operate with a nominal characteristic impedance of 50 Ω.

The key dimensional parameters of the short stub and ground conductor — namely, ground-conductor length (LG), stub length (LS), stub width (WS), and through-hole diameter (DH) — were subjected to comprehensive parametric analysis to determine their influence on impedance matching. Calculated input impedance is plotted as a function of LG in Figure 3, where (a) is the Smith chart, and (b) shows the corresponding reflection characteristics. As LG is increased, the resonance frequency at the higher end of the operating band shifts upward, thereby broadening the overall bandwidth. Concurrently, the quality factor (Q) of the low-frequency resonance tends to increase, while that of the high-frequency resonance decreases, and the resistive component of the input impedance is reduced Calculated input impedance is plotted as a function of LS in Figure 4. Extending the stub length enhances the Q value of the resonance near 3 GHz and shifts the resonance around 5 GHz toward lower frequencies. This variation also leads to an increase in the capacitive component of the input impedance. As a result, the enhanced capacitive contribution counterbalances the inductive component that emerges at reduced antenna dimensions, thereby improving

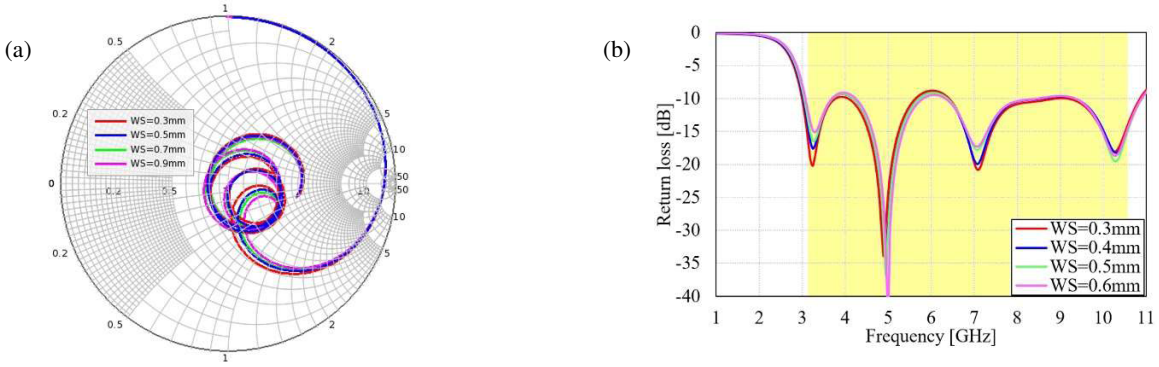

FIGURE 5. Calculated input impedance (with parameter WS): (a) Smith chart (1–11 GHz) and (b) reflection characteristic.

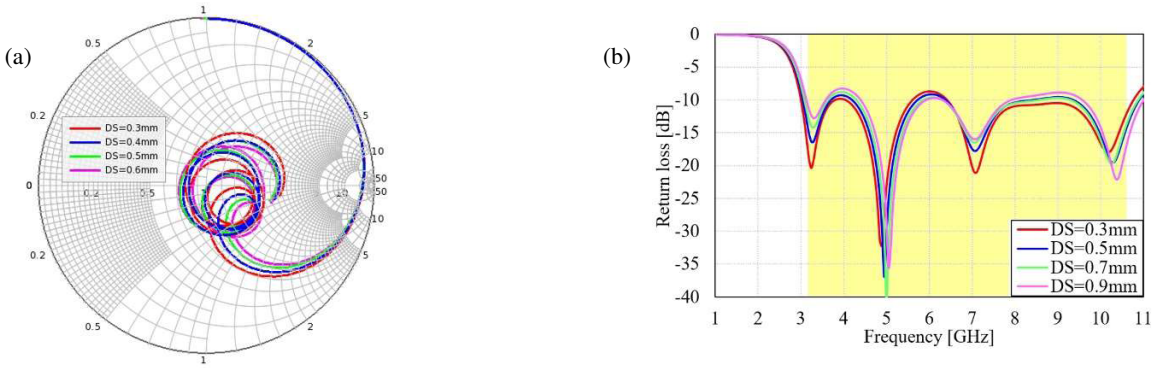

FIGURE 6. Calculated input impedance (with parameter DS): (a) Smith chart (1–11 GHz) and (b) reflection characteristic.

impedance matching at the lower band edge around 3.1 GHz. The input-impedance response is plotted as a function of WS in Figure 5. Increasing stub width reduces the resonant Q values across all resonances while simultaneously reducing the capacitive component of input impedance. Input impedance is plotted as a function of DS in Figure 6. Enlarging through-hole diameter reduces the Q value of the resonance near 3 GHz shifts the resonance around 5 GHz toward higher frequencies, and increases the capacitive component of the input impedance.

The above-described results confirm that the input impedance of the antenna can be effectively tailored by adjusting LG, LS, WS, and DS. By optimizing these parameters to the reference values summarized in Table 1, it is possible to obtain wideband impedance characteristics fully covering the UWB operating range of 3.1–10.6 GHz.

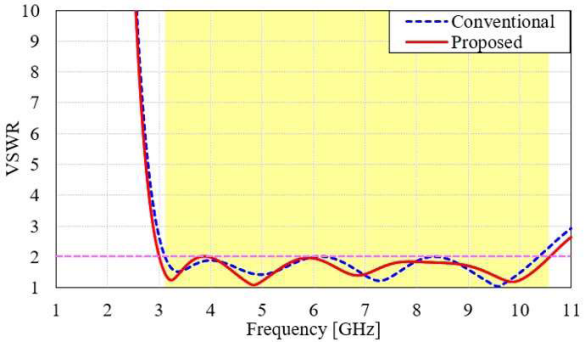

FIGURE 7. Comparison of calculated VSWR.

3. EVALUATION RESULTS

Based on the results of the parametric analysis presented in Section 2, the optimal dimensions of the proposed antenna are determined. The effectiveness of the proposed half-shaped, planar UWB monopole antenna was validated by a comprehensive set of evaluations combining full-wave electromagnetic simulations with experimental measurements of a fabricated prototype. The antenna was fabricated on an FR-4 substrate ($\varepsilon r = 4.4/\tan\delta = 0.02$) with dimensions of $L = 30$ mm, $W = 12$ mm, and $t = 1.6$ mm. A Keysight EMPro electromagnetic field simulator, with the design parameters set to the reference values listed in Table 1, was used for the numerical simulations. The evaluation covered both frequency and domain performances (VSWR, impedance characteristics, radiation patterns, and current distribution) and experimental verification in a manner that ensured that the antenna's simulated performance is reproducible in practice.

3.1. Simulated VSWR Characteristics

The simulated voltage standing-wave ratio (VSWR) characteristics of the proposed antenna are plotted in Figure 7. For comparison, the figure also includes the VSWR curve (shown as a dotted line) of the previously reported bell-shaped monopole antenna with a short stub [22]. The comparison reveals that despite its reduced radiator area, the half-shaped monopole maintains broadband performance almost equivalent to that of the full-shape design. Specifically, the proposed antenna achieves VSWR of ≤ 2 across the entire UWB (from 3.1 to 10.6 GHz).

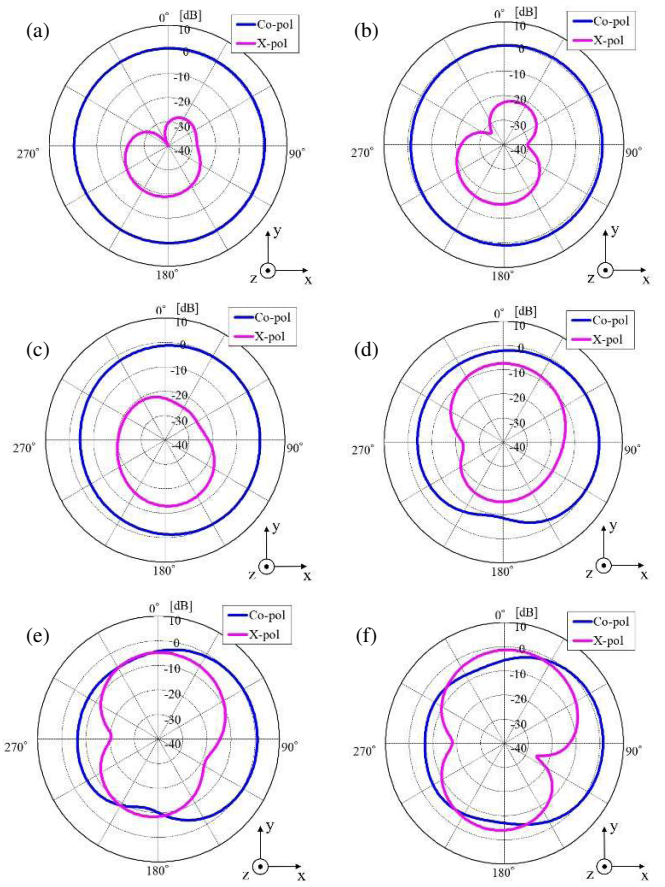

FIGURE 8. Calculated radiation patterns: (a) 3.5 GHz, (b) 4.5 GHz, (c) 6.5 GHz, (d) 8 GHz, (e) 9 GHz, and (f) 10 GHz.

The lower edge of the UWB (around 3.1 GHz) is often challenging to cover (i.e., provide VSWR of $\leq$ 2), particularly in regard to compact antennas, due to the reduced physical dimensions. As for this antenna design, however, the integration of the short stub sufficiently compensates capacitance, thereby ensuring sufficient impedance matching at low frequencies. At the upper end of the UWB ($>$ 9 GHz), the half-shaped radiator still sustains the higher-order resonances necessary for wideband operation. This result confirms that bandwidth is not compromised even when the antenna is half-shaped. A quantitative comparison with the full bell-shaped monopole reported in [22] shows that bisecting the radiator does not reduce the achievable bandwidth. Although the radiator area decreases by about 36% (from $28\times20\,\text{mm}^2$ to $30\times12\,\text{mm}^2$), the proposed half-shaped structure retains the same UWB impedance bandwidth of 3.1–10.6 GHz (VSWR $\leq$ 2). These results confirm that the combination of the monopole and short stub compensation mechanism effectively preserves the lower-band matching and higher-order resonances necessary for wideband behavior.

3.2. Simulation of Radiation Pattern

The radiation characteristics of the proposed antenna were simulated at frequencies of 3.5, 4.5, 6.5, 8, 9, and 10 GHz. The simulated far-field radiation patterns in the x-y plane of the antenna are shown in Figure 8. Across the entire band, the antenna produces nearly omnidirectional radiation patterns and

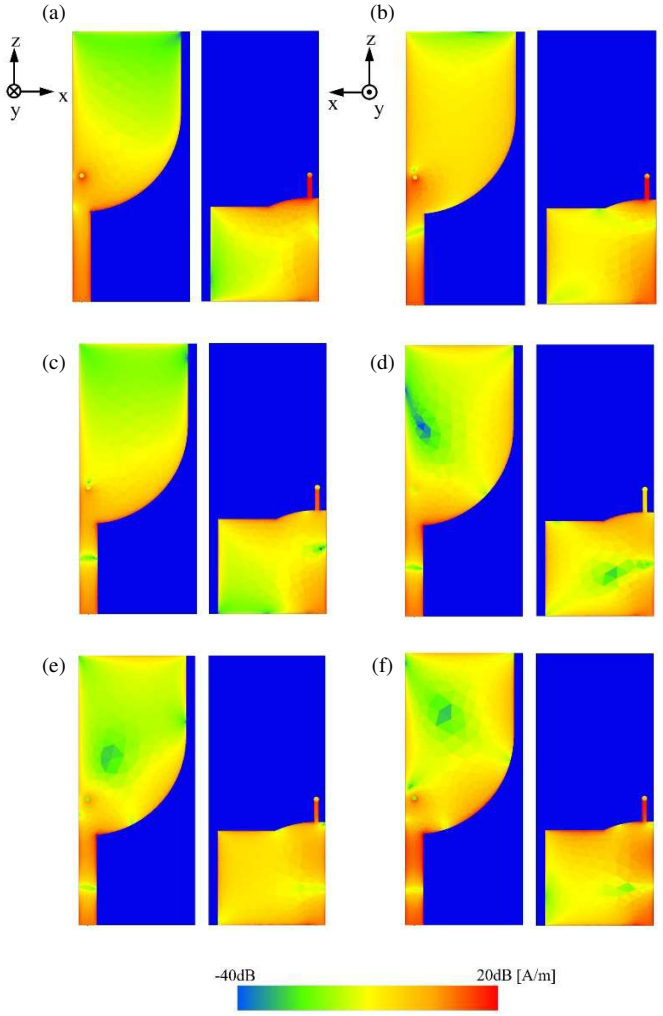

FIGURE 9. Calculated of current distribution (xz plane): (a) 3.5 GHz, (b) 4.5 GHz, (c) 6.5 GHz front view, (d) 8 GHz, (e) 9 GHz, and (f) 10 GHz.

thereby satisfies a critical requirement for UWB communication systems intended for portable and handheld devices. Although a slight tilt of the radiation pattern toward the positive x-axis is observed at higher frequencies (above 8 GHz), the overall radiation behavior remains quasi-omnidirectional. This result indicates that the antenna is capable of supporting stable communication links in environments where device orientation may vary. The radiation patterns also show consistent co-polarization dominance; namely, cross-polarization level remains low throughout the frequency band.

3.3. Analysis of Current Distribution

To elucidate the operating principle of the proposed antenna, the surface current distributions on the monopole at frequencies of 3.5, 4.5, 6.5, 8, 9, and 10 GHz were analyzed, and the analysis result is shown in Figure 9. At 3.5 GHz, current density is concentrated predominantly along the short stub and the lower part of the monopole. This result confirms that the stub plays a vital role in achieving impedance matching at low frequencies. At 6.5 GHz, the current distribution becomes more uni-

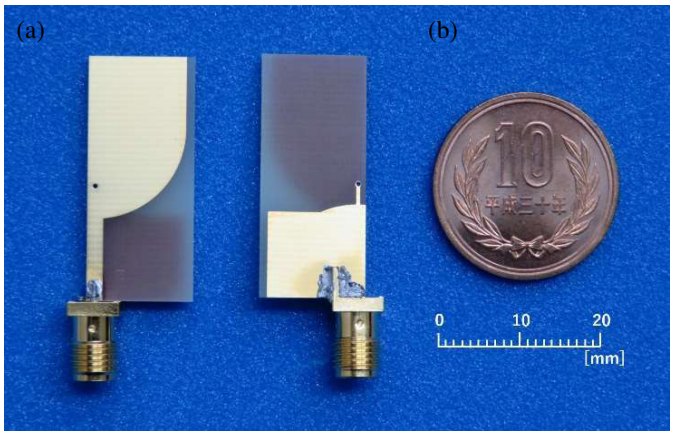

FIGURE 10. Prototype antenna: (a) front view and (b) back view.

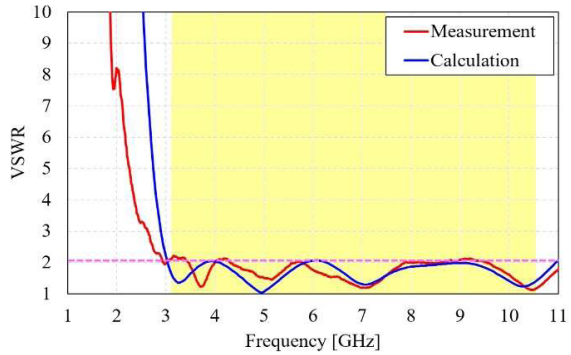

FIGURE 11. Comparison of VSWR.

form across the radiator surface, and the stub is moderately excited. At 10 GHz, the current shifts toward the edges of the radiator, and higher-order modes dominate. Although the stub contribution is weaker at this frequency, its influence on the overall impedance remains evident. These results confirm the physical interpretation provided by the equivalent circuit model, namely, the short stub functions as a parallel capacitive path that compensates the monopole inductance at low frequencies, while at higher frequencies, the monopole itself sustains the resonance of the monopole.

3.4. Prototype Fabrication and Measurement Results

A prototype antenna based on the optimized parameters summarized in Table 1 was fabricated on an FR-4 substrate. The fabricated antenna is shown in Figure 10. An SMA connector was soldered to the feed point for measurement purposes. The input reflection coefficient (S11) and corresponding VSWR characteristics were measured with a vector network analyzer (VNA). The measured VSWR, along with the simulated VSWR for comparison, is plotted in Figure 11. It can be seen that the measurement results agree closely with the calculated results in a manner that confirms the validity of the antenna design. Both figures indicate that the antenna maintains a VSWR of $\leq$ 2 across the entire UWB (from 3.1 to 10.6 GHz). Slight deviations between measured and simulated curves can be attributed to fabrication tolerances (e.g., precision of via diameter and soldering of the SMA connector). Nonetheless, these discrepancies are minimal and do not significantly affect the overall impedance bandwidth of the proposed antenna. The measured radiation patterns of the antenna are shown in Figure 12. The measurement frequencies are the same as those used for calculating the radiation patterns shown in Figure 8. The radiation patterns (co-polarization and cross-polarization) are plotted along the x-y plane.

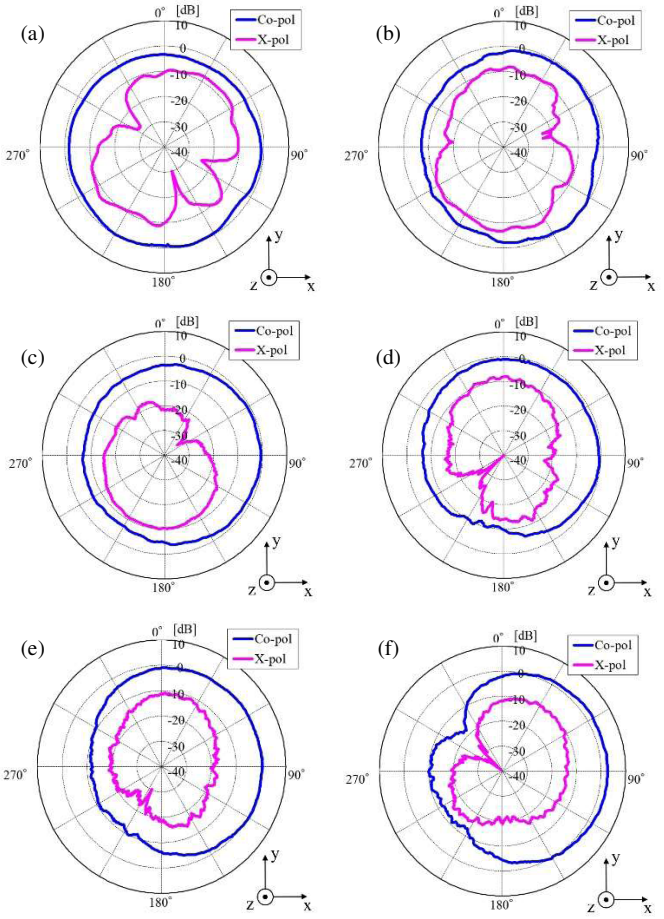

FIGURE 12. Measured radiation patterns: (a) 3.5 GHz, (b) 4.5 GHz, (c) 6.5 GHz, (d) 8 GHz, (e) 9 GHz, and (f) 10 GHz.

These results confirm that the proposed antenna successfully achieves the dual objectives of antenna miniaturization and broadband performance. Compared with the area of the previously reported full-shaped monopole, the antenna area is reduced by approximately 36%, while nearly identical bandwidth characteristics are maintained. The radiation patterns are quasi-omnidirectional across the entire UWB in a manner that ensures robust system-level performance for UWB applications.

4. TIMEDOMAIN ANALYSIS

As for ultra-wideband (UWB) systems, communication is achieved by transmitting digital signals converted into impulse-type or non-sinusoidal waveforms, typically consisting of sub-nanosecond pulses. When transformed into the frequency domain, these signals occupy a bandwidth of several gigahertz. To ensure reliable high-speed communication,

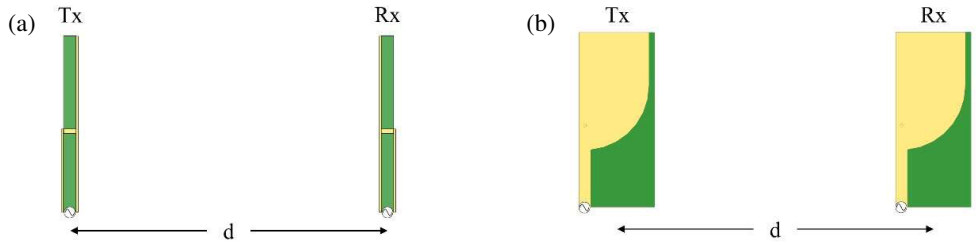

FIGURE 13. Antenna configuration: (a) face-to-face and (b) side-by-side.

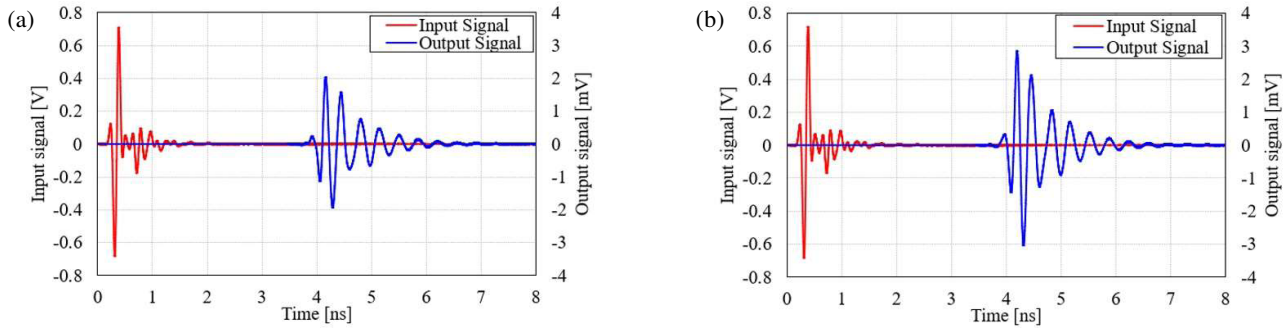

FIGURE 14. Results of time-domain analysis: (a) face-to-face and (b) side-by-side.

UWB antennas must provide stable transmission and reception characteristics that are largely independent of orientation. Consequently, the time-domain fidelity of the antenna becomes just as important as its frequency-domain impedance and radiation characteristics. In practical terms, even if an antenna exhibits wide impedance bandwidth in the frequency domain, poor phase linearity or group delay variation can distort the transmitted waveform, and that distortion leads to inter-symbol interference and reduced data throughput. Therefore, in addition to VSWR and radiation-pattern analysis, time-domain analysis is essential for confirming that the antenna can transmit and receive UWB pulses with minimal distortion.

4.1. Evaluation Methodology

To investigate the time-domain behavior of the proposed antenna, two identical antennas were used as a transmitting (Tx) and a receiving (Rx) pair. The antennas were placed at a distance of 1 m in two different configurations: (a) face-to-face, in which the radiating surfaces are aligned along the same axis, and (b) side-by-side, in which the antennas are oriented in parallel but displaced laterally. These two antenna configurations are illustrated in Figure 13. The distance of 1 m was selected to approximate a typical short-range indoor communication scenario while ensuring operation in the antenna's far-field region at most frequencies within the UWB. A Gaussian pulse is used as the excitation signal. The received signals were recorded, and their temporal waveforms were compared with the transmitted signal to evaluate signal distortion and correlation performance.

4.2. Results of Time-Domain Analysis of Received Waveforms

The results of the time-domain analysis are shown in Figure 14, where (a) corresponds to the face-to-face configuration and (b) corresponds to the side-by-side configuration. A comparison of the two configurations reveals that the received amplitude is approximately 1 mV higher for the side-by-side configuration than for the face-to-face one. This difference in received amplitude is attributed to the slight tilt of the radiation pattern observed in the frequency-domain simulations (Figure 8), where the main lobe exhibits a directional bias toward the positive x-axis at higher frequencies. This directional tendency explains the slightly stronger reception in the case of the side-by-side configuration.

To quantify waveform similarity, the correlation coefficient (ρ) between transmitted and received signals is calculated as

$$\rho = \max_{\tau} \left\{ \frac{\int S_1(t) S_2(t-\tau) dt}{\sqrt{\int S_1^2(t) dt} \sqrt{\int S_2^2(t-\tau) dt}} \right\} \tag{1}$$

where $S(t)$ represents the signal strength, and τ is the delay time. In the case of the face-to-face and the side-by-side antenna configurations, the correlation coefficients are calculated to be 0.986 and 0.929, which confirms a high degree of similarity between the waveforms. Furthermore, in the case of both configurations, the arrival times of the signals are nearly identical. These results demonstrate that the proposed antenna maintains robust time-domain performance and can provide consistent communication quality regardless of the relative orientation of transceivers in UWB applications.

4.3. Group-Delay Characteristics

The group-delay characteristics of the proposed antenna were determined as follows. Group delay, defined as the derivative

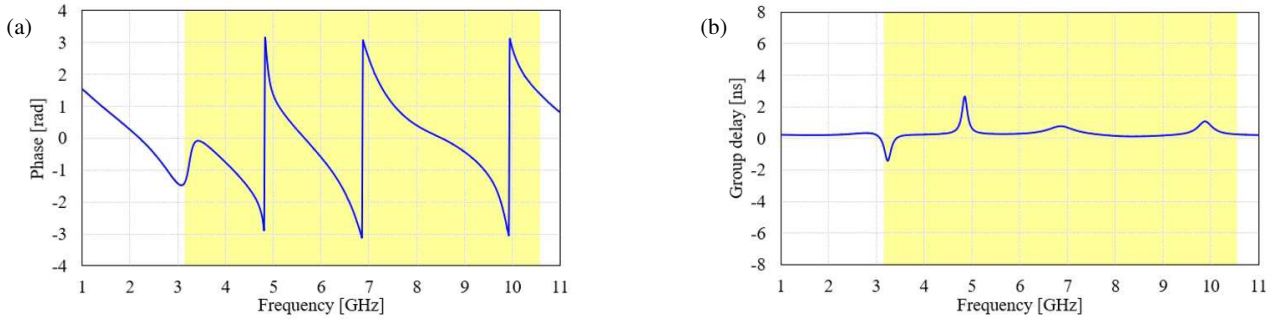

FIGURE 15. Calculated phase and group-delay characteristics of S_{11}: (a) phase and (b) group delay.

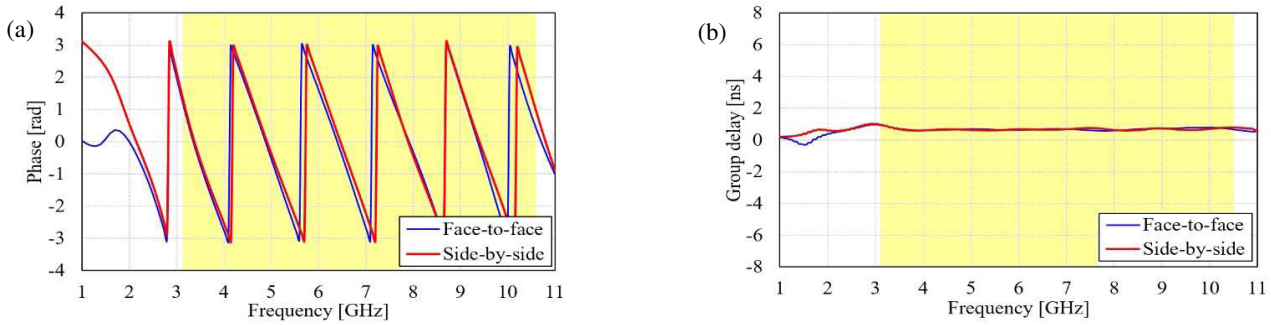

FIGURE 16. Calculated phase and group-delay characteristics of S_{21}: (a) phase and (b) group delay.

TABLE 2. Comparison of conventional antennas with the proposed UWB printed-monopole antenna.

Ref.	Design technique	Antenna size	Antenna substrate	BW	Time-domain analysis
[16]	Square-ring slot-shaped	120×100×0.5	RO4003B	3–11	No
[18]	Trapezoidal slot-shaped with via holes	27×29×1.0	$\varepsilon_r = 2.65$	3.0–10.6	No
[19]	Cactus-shaped	28×20×0.35	LCP	2.9–12	No
[20]	Asymmetric slots on radiator	21.6×20.8×1.6	FR-4	2.2–16.5	Yes
[21]	Modified-hexagonal-shaped	25×12.5×1	FR-4	3.1–10.8	Yes
[22]	Triple band-notched monopole	40×29×1.6	FR-4	2.7–11.0	No
[23]	Circularly-polarized UWB (CMA)	30×24×1.6	FR-4	5.7–10.7	Yes
[24]	DGS-based wideband monopole	34×28×1.5	$\varepsilon_r = 2.2$	4.0–18.9	No
[25]	Ring-structured UWB (CMA)	35×30×1.6	FR-4	3.0–11.7	No
[26]	Bell-shaped, short stub	28×20×1.6	FR-4	3.1–10.6	No
This work	Half bell-shaped, short stub	30×12×1.6	FR-4	3.1–10.6	Yes

of the transmission phase with respect to angular frequency, is expressed as

$$T_d = -\frac{d\theta}{d\omega} \tag{2}$$

where θ denotes the antenna phase, and ω denotes the angular frequency. For broadband communication systems, the group-delay response should exhibit minimal variation (i.e., small phase gradient) and approximate linearity, since these features correspond to low distortion and stable signal transmission. The antenna phase is derived from the complex S-parameters as

$$\theta = \tan^{-1}\frac{Im(S)}{Re(S)} \tag{3}$$

where Re(S) and Im(S) represent the real and imaginary components, respectively. The calculated phase response of S_{11} is shown in Figure 15(a), while the corresponding group-delay characteristics obtained from Equations (2) and (3) are shown in Figure 15(b). The phase response exhibits a moderately steep slope immediately following phase inversion; however, it remains predominantly linear across the operating band. Although the group delay slightly increases at frequencies corresponding to resonant points, the overall delay remains nearly constant at approximately 0.2 ns over the entire UWB range. The calculated phase response of S_{21} and the corresponding group-delay characteristics are shown in Figure 16. The overall delay remains nearly constant at approximately 0.8 ns over

the entire UWB range. This stability confirms that the proposed antenna is well suited for high-speed, low-distortion communication applications.

A comparative study of representative UWB printed-monopole antennas reported in the literature and the proposed half-shaped monopole antenna is summarized in Table 2. The antennas are compared with respect to key performance indicators, namely, antenna size, impedance bandwidth, substrate material, and notable structural features used to achieve broadband characteristics. According to this comparison, many previously reported designs use conventional circular or elliptical monopoles, often combined with slots, tapered structures, or corrugated geometries to extend impedance bandwidth. While these approaches are effective in achieving wide operating ranges, they generally require larger substrate areas and more complex fabrication processes.

In contrast, the proposed half-shaped, printed-monopole antenna achieves comparable or superior performance while having a significantly smaller footprint ($30\times12\times1.6$ mm) and relies solely on a standard FR-4 substrate, which is both low cost and widely available. The adoption of a short stub connected via a through-hole enables effective impedance tuning, particularly at the lower end of the UWB, in which it is typically most difficult to achieve impedance matching with compact designs. This unique approach allows the antenna to maintain VSWR of ≤ 2 across the entire UWB (3.1–10.6 GHz) without introducing excessive structural complexity. Furthermore, unlike several compact UWB antennas that suffer from distorted radiation patterns at higher frequencies, the proposed antenna maintains nearly omnidirectional radiation across the UWB, which ensures reliable performance for mobile and handheld applications. When time-domain metrics such as correlation coefficient and group delay are also considered, it becomes clear that the proposed antenna demonstrates clear advantages in terms of waveform fidelity and temporal stability.

5. CONCLUSIONS

A compact, half-shaped, planar monopole antenna designed to operate across the ultra-wideband (UWB) frequency spectrum was proposed and evaluated. A detailed parametric analysis of antenna performance demonstrated that by adjusting key structural parameters — ground-plane length, short-stub length and width, and through-hole diameter — the antenna's input impedance can be effectively tuned, thereby enabling wideband operation that fully covers the UWB range. It also demonstrated that the proposed antenna provides nearly omnidirectional radiation characteristics. Time-domain evaluations confirmed high signal fidelity, namely, correlation coefficients of 0.986 for both face-to-face and side-by-side antenna configurations. Experimental measurements of a fabricated prototype antenna agreed well with simulation results, verifying that the antenna maintains VSWR of ≤ 2 across the designated UWB. Owing to its compact dimensions and robust frequency- and time-domain performance, the proposed antenna constitutes a promising solution for high-speed, short-range, wireless communication applications.

REFERENCES

[1] Xu, H. and L. Yang, "Ultra-wideband technology: Yesterday, today, and tomorrow," in *2008 IEEE Radio and Wireless Symposium*, 715–718, Orlando, FL, USA, Jan. 2008.

[2] Win, M. Z., D. Dardari, A. F. Molisch, W. Wiesbeck, and J. Zhang, "History and applications of UWB [scanning the issue]," in *Proceedings of the IEEE*, Vol. 97, No. 2, 198–204, Feb. 2009.

[3] FCC, "First Report and Order on Ultra-Wideband Technology," Feb. 2002.

[4] Pyndiah, R., "An overview of UWB technology," in *2006 IET Seminar on Practical Applications for Wireless Networks*, 65–80a, Paris, France, 2006.

[5] Kiminami, K., A. Hirata, and T. Shiozawa, "Double-sided printed bow-tie antenna for UWB communications," *IEEE Antennas and Wireless Propagation Letters*, Vol. 3, 152–153, 2004.

[6] Liang, J., C. C. Chiau, X. Chen, and C. G. Parini, "Study of a printed circular disc monopole antenna for UWB systems," *IEEE Transactions on Antennas and Propagation*, Vol. 53, No. 11, 3500–3504, Nov. 2005.

[7] Agrawall, N. P., G. Kumar, and K. P. Ray, "Wide-band planar monopole antennas," *IEEE Transactions on Antennas and Propagation*, Vol. 46, No. 2, 294–295, Feb. 1998.

[8] Evans, J. A. and M. J. Amunann, "Planar trapezoidal and pentagonal monopoles with impedance bandwidths in excess of 10 : 1," in *IEEE Antennas and Propagation Society International Symposium. 1999 Digest. Held in conjunction with: USNC/URSI National Radio Science Meeting (Cat. No.99CH37010)*, Vol. 3, 1558–1561, Orlando, FL, USA, Jul. 1999.

[9] Taniguchi, T. and T. Kobayashi, "An omnidirectional and low-VSWR antenna for the FCC-approved UWB frequency band," in *IEEE Antennas and Propagation Society International Symposium. Digest. Held in conjunction with: USNC/CNC/URSI North American Radio Sci. Meeting (Cat. No.03CH37450)*, Vol. 3, 460–463, Columbus, OH, USA, Jun. 2003.

[10] Su, S.-W., K.-L. Wong, and C.-L. Tang, "Ultra-wideband square planar monopole antenna for IEEE 802.16 a operation in the 2–11-GHz band," *Microwave and Optical Technology Letters*, Vol. 42, No. 6, 463–466, 2004.

[11] Antonino-Daviu, E., M. Cabedo-Fabrés, M. Ferrando-Bataller, and A. Valero-Nogueira, "Wideband double-fed planar monopole antennas," *Electronics Letters*, Vol. 39, No. 23, 1635–1636, Nov. 2003.

[12] Wong, K.-L., C.-H. Wu, and S.-W. Su, "Ultrawide-band square planar metal-plate monopole antenna with a trident-shaped feeding strip," *IEEE Transactions on Antennas and Propagation*, Vol. 53, No. 4, 1262–1269, Apr. 2005.

[13] Srifi, M. N., S. K. Podilchak, M. Essaaidi, and Y. M. M. Antar, "Planar circular disc monopole antennas using compact impedance matching networks for ultra-wideband (UWB) applications," in *2009 Asia Pacific Microwave Conference*, 782–785, Singapore, Dec. 2009.

[14] Koshiji, F., S. Itaya, Y. Akiyama, and K. Koshiji, "Proposal and investigation of miniaturizing unbalanced dipole antenna for ultra wideband radio," *Journal of The Japan Institute of Electronics Packaging*, Vol. 15, No. 7, 526–533, Nov. 2012.

[15] Abbosh, A. M., "Miniaturization of planar ultrawideband antenna via corrugation," *IEEE Antennas and Wireless Propagation Letters*, Vol. 7, 685–688, 2008.

[16] Sadat, S., M. Fardis, F. Geran, G. Dadashzadeh, N. Hojjat, and M. Roshandel, "A compact microstrip square-ring slot antenna for UWB applications," in *2006 IEEE Antennas and Prop-*

agation Society International Symposium, 4629–4632, Albuquerque, NM, USA, Jul. 2006.

[17] Azim, R., M. T. Islam, and N. Misran, "Compact tapered-shape slot antenna for UWB applications," *IEEE Antennas and Wireless Propagation Letters*, Vol. 10, 1190–1193, Oct. 2011.

[18] Chen, D. and C.-H. Cheng, "A novel compact ultra-wideband (UWB) wide slot antenna with via holes," *Progress In Electromagnetics Research*, Vol. 94, 343–349, 2009.

[19] Nikolaou, S. and M. A. B. Abbasi, "Miniaturization of UWB antennas on organic material," *International Journal of Antennas and Propagation*, Vol. 2016, No. 1, 5949254, 2016.

[20] Kempanna, S. B., R. C. Biradar, T. Ali, V. K. Jhunjhunwala, S. Soman, and S. Pathan, "A Compact slotted UWB antenna based on characteristics mode theory for wireless applications," *Designs*, Vol. 7, No. 6, 141, Dec. 2023.

[21] Park, S. and K.-Y. Jung, "Novel compact UWB planar monopole antenna using a ribbon-shaped slot," *IEEE Access*, Vol. 10, 61 951–61 959, Jun. 2022.

[22] Lin, H., Z. Lu, Z. Wang, and W. Mu, "A compact UWB monopole antenna with triple band notches," *Micromachines*, Vol. 14, No. 3, 518, 2023.

[23] Heo, H., M.-J. Kang, S. Park, J. Lee, L. Qu, and K.-Y. Jung, "Design of a UWB circularly-polarized planar monopole antenna using characteristic mode analysis," *Scientific Reports*, Vol. 14, No. 1, 26236, 2024.

[24] Tsegaye, A., X.-Q. Lin, H. Liu, and H. S. Abubakar, "A compact monopole wideband antenna based on DGS," *Electronics*, Vol. 14, No. 12, 2311, 2025.

[25] Xiang, Z., Z. Wang, C. Li, and R. You, "Design of UWB monopole antenna with ring structure based on characteristic mode theory," *Progress In Electromagnetics Research C*, Vol. 158, 225–234, 2025.

[26] Takemura, N. and S. Ichikawa, "Broadbanding of printed bell-shaped monopole antenna by using short stub for UWB applications," *Progress In Electromagnetics Research C*, Vol. 78, 57–67, 2017.

[27] Ichikawa, S. and N. Takemura, "A study on half-shaped printed monopole antenna with short stub for UWB system," *IEICE Communications Express*, Vol. 9, No. 6, 213–217, Jun. 2020.

[28] Pele, I., A. Chousseaud, and S. Toutain, "Simultaneous modeling of impedance and radiation pattern antenna for UWB pulse modulation," in *IEEE Antennas and Propagation Society Symposium, 2004.*, Vol. 2, 1871–1874, Monterey, CA, USA, Jun. 2004.